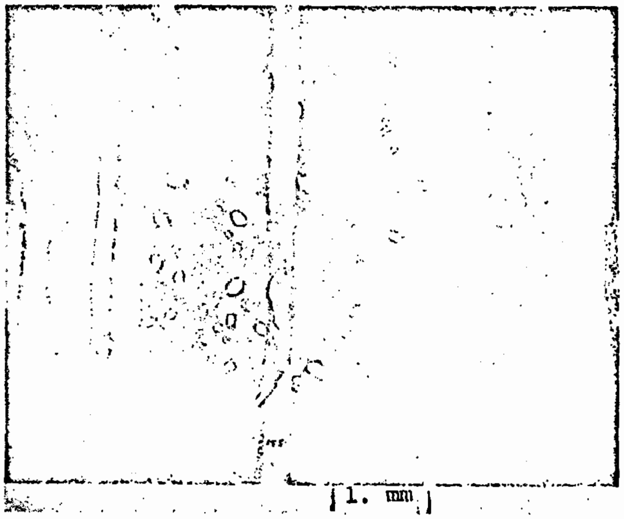

FIG. 4. Large "splatter" image from graupel probably slightly "mushy." Most of the 25- to 200-μ images appear to be from liquid, but some appear as ice fragments.

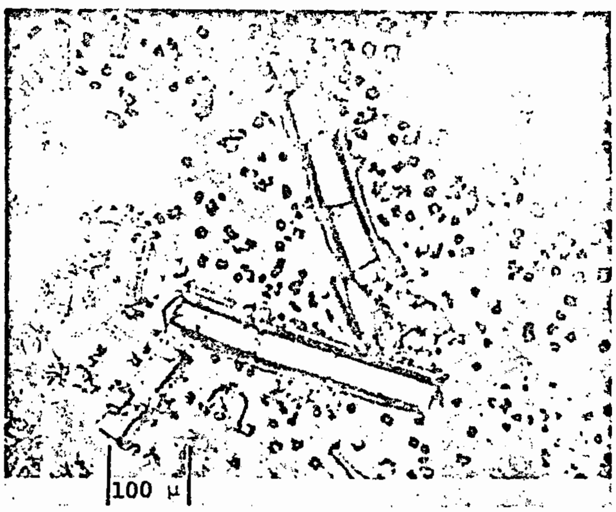

FIG. 5. Images typical of many 40- to 60-μ hexagonal columns. Dark areas are "blush." Spurious crystal growth is distinguishable from the original small shatter fragments.

rate, between the points of coating application and droplet impaction. The viscosity is about doubled by a 15C lowering of the temperature or a 2 per cent increase in the concentration (at 8 per cent). The viscosity of the liquid coating at the time of impaction affects the character of the resultant images in several respects, including the amount of "cushioning" (hence, break-up on impact), the amount of droplet flattening [hence, the size of image for a given droplet size (MacCready and Todd, 1964)], the relative number of droplets replicated (collection efficiency), coalescence of the drops on the film during the period of impaction but prior to encapsulation, and the range of droplet sizes which are encapsulated as compared to those forming open replicas. In the case of ice crystals the viscosity also affects the preservation of the replica shapes during the time when the ice is melting upon entering the heater.

Thickness of coating. The coating thickness also affects all of the above, as well as the drying time, the density of color (if dye is used), and the amount of "blush" (discussed later) formed for a given humidity of the drying air and the time at each temperature used in the drying process. The present design of applicator which uses the pressure-coating method provides a coating thickness that is nearly independent of the viscosity and fluid pumping rate. With this design, viscosity and pumping rate mainly affect the width of the coating on the film and whether or not excess fluid drains away. In order to obtain usable replication over a range of conditions the coating is applied with gradations of thickness across the film as can be seen in Fig. 4.

Coating applicator. The Formvar solution is pumped onto the film through a "fountain pen" which is designed so that hardened Formvar from a previous run is

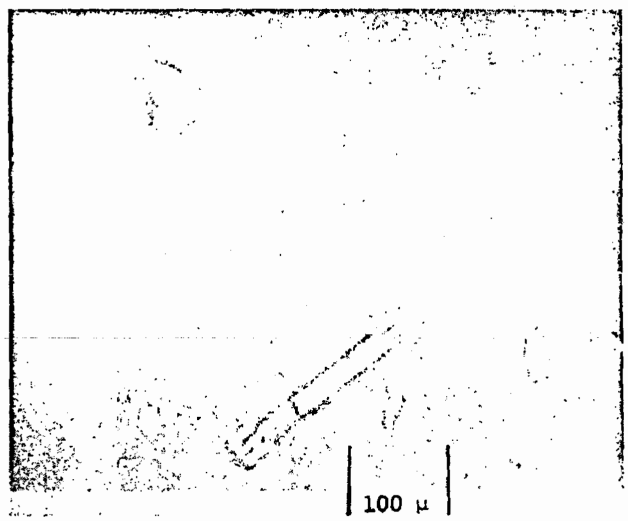

FIG. 6. Hexagonal column 50 μ across and fragments apparently from 150-μ thin-wall hexagonal column.

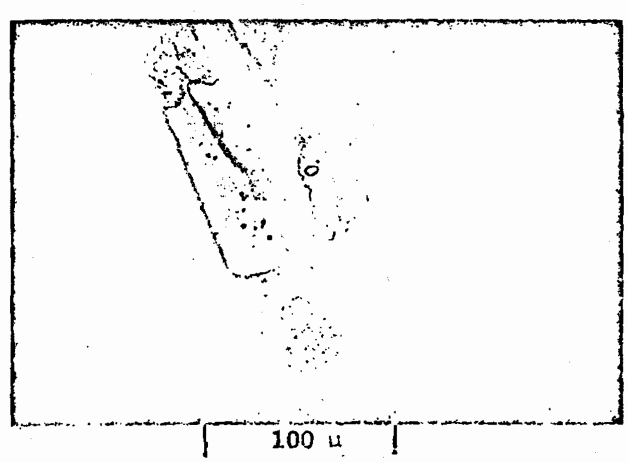

FIG. 7. Hexagonal column 60 μ across showing replica of hollow cross section.

bypassed by expansion of the "pen" under the pressure built up by the metering pump. The solvent gradually softens the hard portion, permitting the expansion to decrease. The point of the "pen" incorporates a 7 mm wide scraper plate which has various depth notches. The Formvar is thereby spread across the film in various thicknesses, any excess forming an extra ridge beyond the edges of the scraper.

Entry port configuration. The entry port configuration limits the minimum distance along the film from the applicator to the sample air entry port. The proximity of the applicator to the sampling point influences the amount of evaporation, hence the thickness and viscosity of the Formvar surface. The applicator can be located as close as 1 cm to the sampling point if the film is passed around a cylindrical roller at the entry port.

1) Collection efficiency.

The efficiency of collection of various sizes of droplets by different aerodynamic shapes moving at various air speeds is discussed by Langmuir and Blodgett (1945). With an aerodynamically leading surface in the form of a flat plate, the collection efficiency for small droplets on that surface is lower than it is for a cylinder of equal size.

Collection efficiency calculations for simple cylinders and flat plates, as presented by Langmuir and Blodgett (1945), are not applicable when the surface contains a sampling entry or slot, since the back pressure and the trajectories of droplets are changed by the presence of the slot. The collection efficiency at the film may be either higher or lower than that calculated for a continuous flat plate or cylinder. With the film located behind the slot, the slot acts as an orifice so that the air and droplet velocity at the film surface is lower than the velocities used in the collection efficiency calculations of Langmuir and Blodgett. Simple proof that the air velocity is lower with a narrower entry slot was found when attempts were made to fly a unit with a larger entry (reducing the diffusing effect of the slot). In that flight experiment, even with aircraft speeds as low as 120 mph, much of the Formvar coating was blown off the film.

2) Coalescence and drop shattering.

At airspeeds as high as the 265 mph of the Super-constellation (at 17,000 ft) with a 2-mm slot and a flat-plate type of leading surface, one of the limitations of the instrument is the excessive number of replicas overlapping each other, leading to difficulty in obtaining meaningful photomicrographs. The less dense regions of the clouds were used for all of Figs. 2–7 in order to improve clarity in identification of the various types of cloud particles. The replicas from more dense (and hence more representative) portions of the clouds were included in the data reduction for other types of analysis.

Several types of particle entry ports have been used in attempts to reduce shattering and excessively high

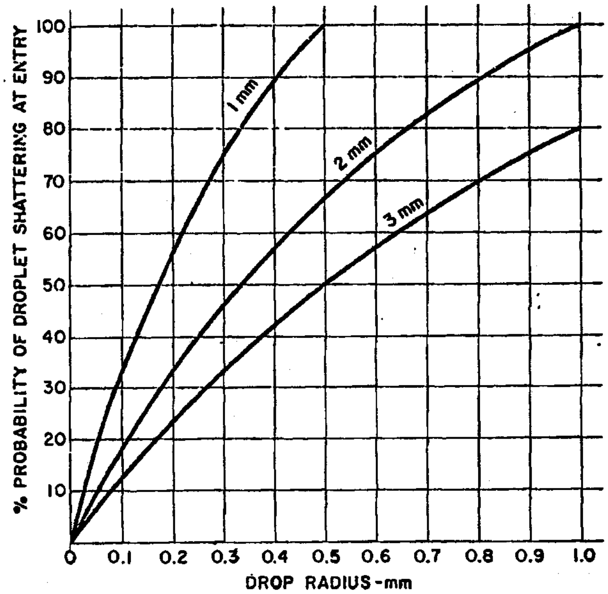

Fig. 8. Probability of various radii drops overlapping the edges of 1, 2, and 3 mm wide entry ports, computed on geometrical basis without corrections for spattering from drops entirely outside entry or for small droplets not shattering when touching entry edge.

concentrations of droplets reaching the film. The high concentration can result in coalescence of the droplets to produce large images when actually no large drops are present (particularly in high-water-content clouds). On the flights discussed in the accompanying article (Ruskin, 1967), the sampling time of about 0.01 sec was sufficient to cause coalescence on the film. In an attempt to reduce the uncertainties caused by this problem the sampling port was tapered from 3 mm wide at one edge of the film to zero width at the other edge. The wide part of the sampling port permitted large droplets and ice crystals to enter with relatively few being shattered or spattered by the edges of the port. The narrow edge provided a shorter exposure time. Although the density of replicas is not entirely proportional to port width at various locations across the film, comparison of the sizes and concentrations near the opposite edges of the film gives a clue as to the amount of shattering and coalescence. Fig. 8 shows the probability of various drop sizes hitting the edges of the sampling port for the cases of a 1-, 2-, and 3-mm width of the port. Fig. 8 is based on the assumptions 1) that all drops overlapping an edge are shattered and 2) that no fragments enter when shattered drops are entirely outside of the port. Because of departures from 1) the values of probabilities shown on the curves are probably somewhat too high for radii below about 50 μ. Departures from 2) probably cause the values to be underestimated for large drops.

Other entry configurations are under study with the aim of reducing the uncertainties in image interpretation.

contents with these aircraft speeds the images were too crowded and coalesced to permit quantitative interpretation. So many factors affect the collection efficiency that before a large effort is expended in calibrations all of the other variables should be optimized and then not changed.

4. Conclusions

In the use of this instrument care must be taken to avoid conclusions drawn from ambiguities in the replicas produced, the uncertainties increasing at higher aircraft speeds. The instrument can provide data which are essentially unobtainable by other means, namely, profiles through clouds giving information as to whether the cloud particles are ice or water, the changes in their ratios, and information about the nature of the ice particles.

The instrument was used in tropical cumulus at −3 to −5C leading to the following results:

1) Replicas were obtained at −3 to −5C of hexagonal column ice crystals, 40 to 60 μ across, some of which had hollow centers.
2) Evidence was found that thin-walled hexagonal columns 150 μ across were prevalent, although all were shattered upon impact at 260 mph. Much ice was present at −5C in spheres as small as 5 μ.
3) Some needles 5 μ across appeared to have grown from one side of 7-μ spheres.

Evidence was found that some hexagonal columns terminated on both ends in points which were extensions of corners of the hexagon. Column length before impact appeared to have been about 300 μ.

Development is continuing toward providing a geometry of sampling entry which is satisfactory at speeds above 50–80 m sec^{-1}.

Acknowledgments. In the N.R.L. phases of the development of the cloud particle replicator, Messrs. R. M. Schecter and R. G. Russ performed most of the flight testing.

The enthusiasm and cooperation of Mr. Clem Todd over a number of years has been a large factor in the instrument having reached its present state of development.

REFERENCES

Braham, R. R., Jr., 1964: What is the role of ice in summer rainshowers? *J. Atmos. Sci.*, **21**, 640–645.

Hallett, J., 1965: Field and laboratory observations of ice crystal growth from the vapor. *J. Atmos. Sci.*, **22**, 64–89.

Kobayashi, T., 1958: On the habit of snow crystals artificially produced at low pressures. *J. Meteor. Soc. Japan*, Series 2, **36**, 193.

Langmuir, I., and K. B. Blodgett, 1945: Mathematical investigation of water droplet trajectories. General Electric Report No. RL-225, Final Report Army Contract W-33-038-ac-9151, 46 pp.

MacCready, P. B., Jr., and C. J. Todd, 1964: Continuous particle sampler. *J. Appl. Meteor.*, **3**, 450–460.

Ruskin, R. E., 1967: Measurements of water-ice budget changes at −5C in AgI-seeded tropical cumulus. *J. Appl. Meteor.*, **6**, 72–81.

Squires, P., 1956: The micro-structure of cumuli in maritime and continental air. *Tellus*, **8**, 443.

——, and S. Twomey, 1966: A comparison of cloud nucleus measurements over Central North America and the Caribbean Sea. *J. Atmos. Sci.*, **23**, 401–404.

Todd, C. J., 1965: Ice crystal development in a seeded cumulus cloud. *J. Atmos. Sci.*, **22**, 70–78.